IOSR Journal of Electronics and Communication Engineering (IOSR-JECE)
e-ISSN: 2278-2834,p- ISSN: 2278-8735.Volume 13, Issue 4, Ver. I (Jul.-Aug. 2018), PP 76-84
www.iosrjournals.org

Design of Compact UWB Microstrip Antenna Using Double-Layer 2D Periodic Structure

Gehad Nady, Ehab K. I. Hamad
Department of Electrical Engineering, Faculty of Engineering, Aswan University Aswan 81542, Egypt
Corresponding Author: Ehab K. I. Hamad

Abstract : *This paper describes a compact ultra-wideband (UWB) antenna designed on a low-cost FR4 substrate using planar-patterned metamaterial concepts. The proposed antenna incorporates two components of metamaterial structure made by etching a T-shaped slots on the main radiating patch and W-shaped slots on the ground plane. The total size of the proposed antenna is 27.6×31.8 mm^2, with a substrate thickness of 1.6 mm, relative permittivity of 4.5, and loss tangent of 0.02. Applying the -10 dB criterion, the 50 Ω impedance bandwidth is from 3.3 GHz to more than 17 GHz, with a standing wave ratio (SWR) of less than 2 over the whole band. The average gain over the entire bandwidth is 5.8 dB, with a peak value of 6.9 dB at 12.2 GHz. The proposed antenna was designed and simulated using the finite integration technique (FIT)-based CST microwave studio. Good agreement between measurement and simulated results was obtained. Thus, the proposed antenna could be applied to UWB wireless communications in the future.*

Keywords: *Antennas, Metamaterials, Microstrip antenna, Periodic structure, Ultra-wideband.*

Date of Submission: 20-08-2018 Date of acceptance: 03-09-2018

I. Introduction

Ultra-wideband (UWB) communication technology has attracted wide attention since the Federal Communication Commission (FCC) released a band of 7.5 GHz (3.1 – 10.6 GHz) as the ultra-wideband in 2002 [1]. UWB is a radio technology widely used in the field of short distance wireless communication as it addresses the demands of bandwidth, cost, and power consumption. The microstrip patch antenna is highly regarded in the design of UWB antennas because of its advantages such as light weight, low volume, low cost, low profile, small dimension, ease of fabrication and conformity as compared with conventional antennas [2]. In terms of bandwidth, patch antennas are considered narrowband. In this regard, several techniques have been proposed to enhance their bandwidth, such as by increasing the height of the substrate, using low permittivity substrate [3], etching slots of different shapes on the radiating patch [4, 5], stacking different antenna elements [6], using parasitic elements around the patch, and using electromagnetic band gap (EBG) structures on the ground plane [7]. A direct technique that widens the bandwidth is achieved by good impedance matching between the feeding line and the radiating element [8]. These techniques equip antennas with wide impedance bandwidth and good radiation performance [9].

Use of metamaterial is another means to improve bandwidth effectively [10]. While there are many definitions for metamaterials [11, 12], they can generally be defined as a class of artificial media that exhibit extraordinary electromagnetic properties not found in nature [11]. Metamaterials are divided into two categories, viz. resonant and non-resonant structures. The first category that is based on unit cells consisting of split ring resonators and wires [13] is less interesting because of its high loss and narrow bandwidth. On the other hand, the second type can be realized directly on a planar transmission line and has potential for use in microwave devices and antennas in the microwave frequency range. The non-resonant type is left-handed material (LHM), which is preferable from the application viewpoint. It is easily manufactured in a planar structure with distinct patterns that are usually formed by repeating a unit cell periodically in such way as to form an array [14].

Some metamaterial-based antennas are reported in the literature [15, 16] to provide good impedance bandwidth and radiation performance. However, they also come with some disadvantages such as size, high-cost substrate used for the antenna but not in PCB circuit design and inadequate coverage of the Federal Communication Commission band (3.1-10.6 GHz). Accordingly, we have taken these factors into consideration in our design process. We note that electromagnetic band gap (EBG) structures consisting of periodic metal patches on a dielectric substrate provide good opportunities to improve antenna characteristics such as antenna gain or bandwidth [17, 18].

The goal of this paper is to propose a new design antenna with wide bandwidth and good radiation performance while remaining compact in size and low in cost. This can be achieved using the inspired double-layer planner periodic geometry of metamaterial structures. The proposed antenna which is modeled using the

finite integration technique (FIT)-based CST microwave studio software provides an impedance bandwidth spreading over from 3.2 GHz to more than 17.5 GHz. The dimensions of the designed antenna are 27.6×31.8 mm^2, with a maximum gain of 6.9 dB. The proposed antenna, with its good radiation characteristics, can be adopted for UWB applications.

The current paper is organized as follows: after an introduction to the current study in Section 1, the design configuration for the proposed antenna is illustrated in Section 2. Some of the major parameters of the proposed antenna geometry are described in Section 3. Final EM simulation with measurement results and discussion are given in Section 4, while the conclusion of this report is presented in Section 5.

II. MTM Unit Cell Configuration

The metamaterial unit cell proposed in this study is divided into two types. The first type is integrated into the radiating patch and all cells are connected together by metal. The second type is to be incorporated on the ground plane and each cell is isolated from the others. As depicted in Fig. 1, 2D periodic structured from the first and the second MTM cells are distributed over the patch and ground plane, respectively. Incorporation of slots within the antenna is a way of enhancing bandwidth in microstrip antennas [19, 20]. In this manner, four T-shaped slots are positioned together to form the unit cell as shown in Fig. 1(a). The cell of slots that is created is then repeated periodically in two dimensions and implemented within the patch. In addition, another four W-shaped slots are positioned together to form another configuration of the MTM unit cell as shown in Fig. 1(b). The created cell is then repeated periodically in two dimensions and implemented within the ground plane. In this manner, the top T-shaped cell is vertically oriented with the bottom cell W-shaped as depicted in Fig. 1(c).

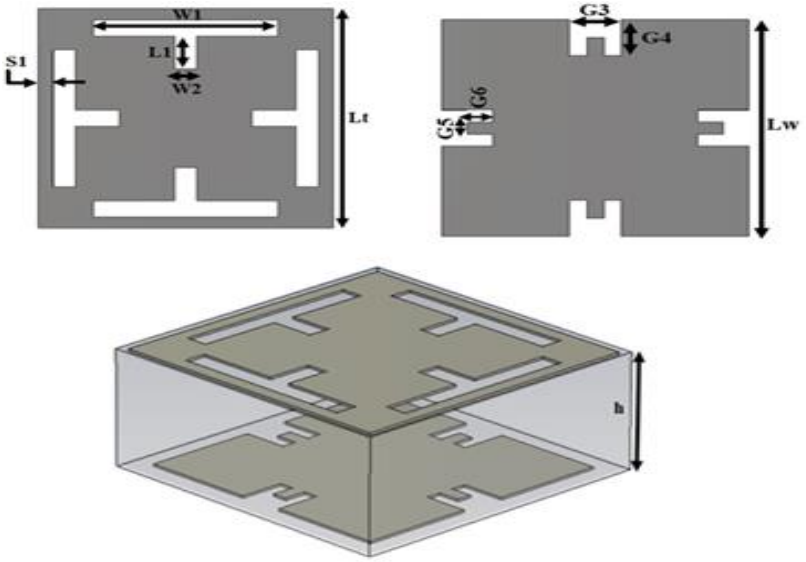

Fig. 1. Schematic diagram of the proposed MTM unit cell, designed parameters Lt = 4, $W1$ = 2.5, $W2$ = 0.3, $L1$ = 0.6, $S1$ = 0.2, Lw = 3.6, $G3$ = 0.6, $G4$ = 0.6, $G5$ = 0.2, $G6$ = 0.3. (All dimensions in mm).

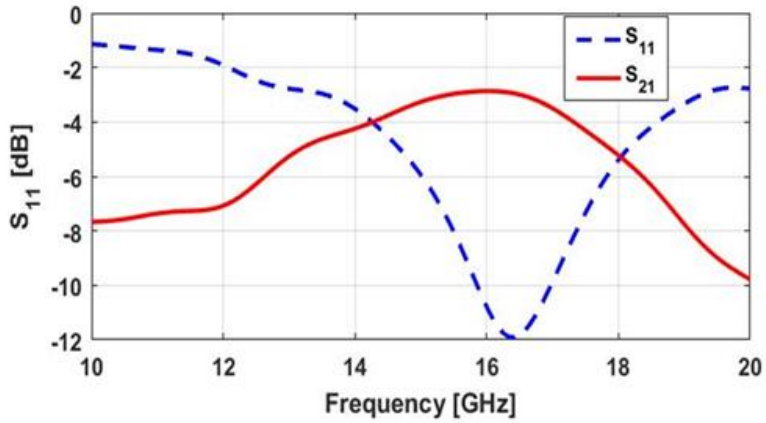

Fig. 2. S-parameter of the unit cell displayed in Fig. 1(c).

To check the operation of the MTM upper unit cell in conjunction with the lower unit cell, one cell shown in Fig. 1(c) was constructed on FR4 substrate with a dielectric constant of 4.5, and loss tangent of 0.02 and height of 1.6 mm with dimensions (mm) *Lt* = 4, *W*1 = 2.5, *W*2 = 0.3, *L*1 = 0.6, *S*1 = 0.2, *Lw* = 3.6, *G*3 = 0.6, *G*4 = 0.6, *G*5 = 0.2, *G*6 = 0.3. The CST Microwave Studio software was used to model the unit cell based on the time domain solver. The S-parameters resulting from the simulation are shown in Fig. 2, where the transmission peak occurred at 16.4 GHz as observed. The unit cell proposed was located between two waveguide ports with perfect electric and magnetic wall boundaries set on it.

The top view of the patch with the 2D periodic pattern is shown in Fig. 3(a), while the bottom view of the ground plane with the second 2D periodic pattern is depicted in Fig. 3(b). The MTM pattern on the ground plane was not created in the area underneath the microstrip feed line to keep the transmission consistency of input energy [21]. The MTM unit cell in the radiating patch and in the ground plane were coupled to form a capacitive-inductive equivalent circuit, which induced a backward wave that traveled along the plane of the patch and induced more radiation in the plane of the antenna.

III. Antenna Design and Configuration

The entire structure of the proposed antenna is constructed with the 2D pattern of the first unit cell incorporated in the top layer (patch) in addition to the 2D pattern of the second unit cell incorporated in the bottom layer (ground plane) as illustrated in Fig. 4. The periodic geometry within the patch consists of an array of 3×4 cells (T-shaped MTM unit cell) while the periodic geometry within the ground consists of 7×6 cells (W-shaped MTM unit cell). The top unit cells are metallically connected together but the bottom unit cells are isolated from one another by surrounding rectangular slots. The physical parameters of the optimized antenna are as follows: *Ws* = 27.6, *Ls* = 31.8, *Wp* = 12, *Lp* = 16, *Wf* = 8, *Lf* = 3, *We* = 15, *Lg* = 8, *G*1 = 0.2, *G*2 = 0.4, all dimensions in mm. The proposed antenna is structured on 1.6 mm-thick FR4 substrate ($\varepsilon r = 4.5$, $\tan\delta = 0.02$) measuring 27.6×31.8 mm^2 in size. The proposed antenna is fed using a 50 Ω microstrip line of 3 mm width to provide good impedance matching. In this antenna design, the radiating patch and ground plane are coupled to form a capacitive-inductive equivalent circuit due to the induced backward wave which travels along the plane of the patch; hence, the radiation along the direction of the patch increases.

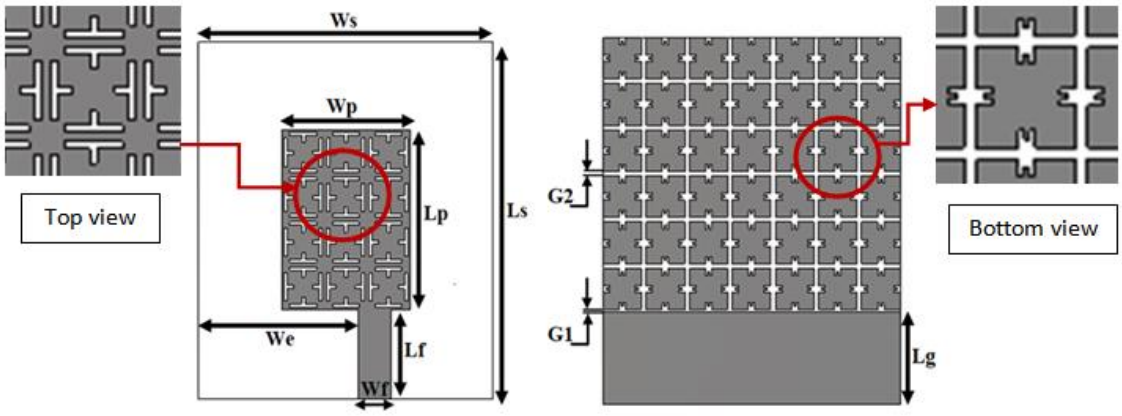

Fig. 3. Geometry of the proposed antenna; W_s = 27.6, L_s = 31.8, W_p = 12, L_p= 16, W_f = 8, L_f= 3, W_e = 15, L_g = 8, G_1= 0.2, G_2= 0.4 (All dimensions in mm.)

IV. Parametric Study

To clearly understand the influence of the antenna parameters on impedance bandwidth, a study on some major design parameters of the antenna was undertaken. When changing one parameter, the other parameters were kept fixed to their optimized values. First, the feed line position of its contact with the patch was taken as a dominant parameter to control the matching properties of the antenna. Three cases (variables) were considered for the distance studied (*We*) before creating the MTM unit cell. The antenna in the first case (*We* = 11 mm) covered the high-frequency regime well, but not so much the low frequencies. The same was true of the second case (*We* = 13 mm). The third case (*We* = 15 mm) covered the low-frequency adequately as shown in Fig. 4. In all cases, the original patch antenna did not cover the band released from FCC. i.e. 3.1 to 10.3 GHz as ultra-wideband, which was why we set out to improve the operating frequency range of the proposed antenna. Having settled on creating the proposed MTM unit cells within the patch and ground plane, another round of study for the above cases was undertaken. A significantly improved bandwidth was achieved by adjusting the feed line position as depicted in Fig. 5.

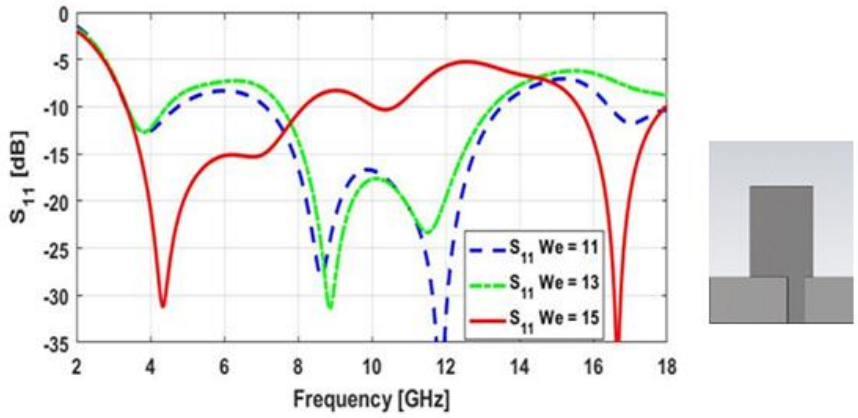

Fig. 4. Effect of changing *we* for a conventional patch antenna

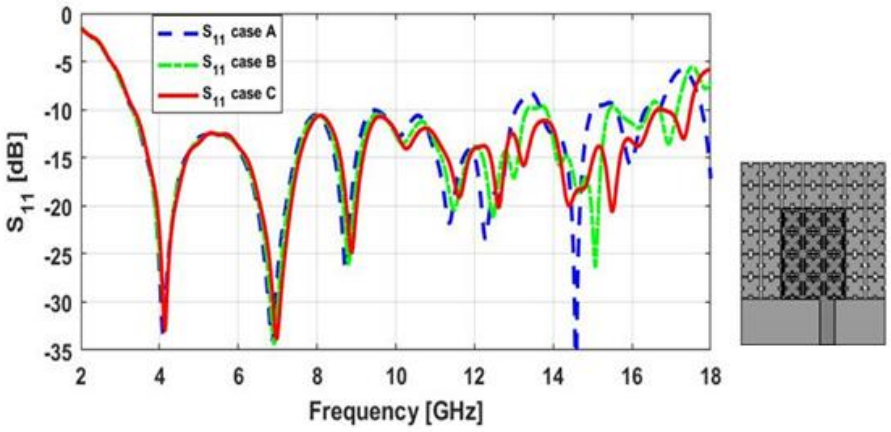

Fig. 5. Effect of changing *we* on the antenna after creating the MTM unit cells top and bottom

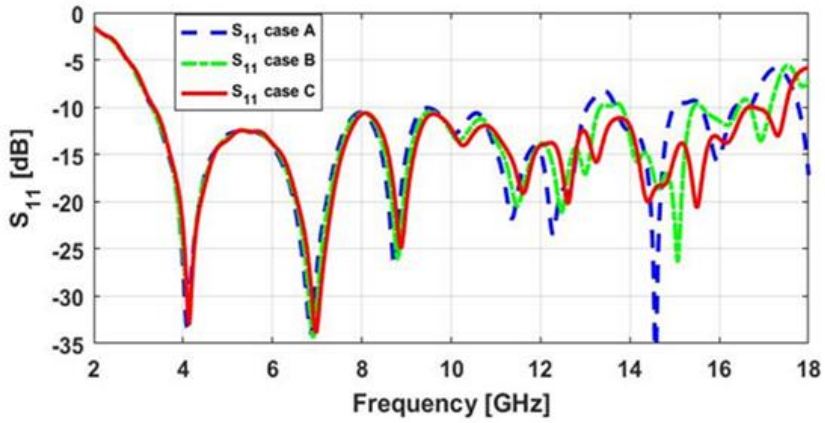

Fig. 6. Parametric study where the values of *G*3 and *G*4 were varied.

Fig. 6 shows three trials of the parameters *G3* and *G4* with the other parameters held constant to examine its impact on bandwidth, viz. Case (A) the parameter *G3* = *G4* = 0.8 mm, case (B) the parameter *G3* = *G4* = 0.7 mm, and case (C) the parameter *G3* = *G4* = 0.6 mm. At a higher value, as in case (A), the bandwidth decreased, whereas with smaller values such as in case B and case C, the bandwidth improved considerably. Hence, the best value for *G3* and *G4* was 0.6 mm. It was not possible to go lower than 0.6 mm because of the constraint in the width of *G3* in relation to *G5*, as shown in Fig. 1 due to the available technology limitations to manufacture the antenna with a slot of less than 0.2 mm width. The frequency

16.7 GHz fell within the band by changing the *G6* value, as shown in Fig. 7. In conclusion, the frequency range was more sensitive to the parameters of unit cells created in the ground plane. The bandwidth improved due to the increases of current paths on the ground. Fig. 8 shows the parametric study of the length *W*1 of the T-shaped slot etched in the patch. As shown, the length of *W*1 had an effect on frequencies around 9.6 GHz to 9.9 GHz. When the length of the slot *W*1 was increased, the frequencies from 9.6 to 9.9 GHz fell within the range.

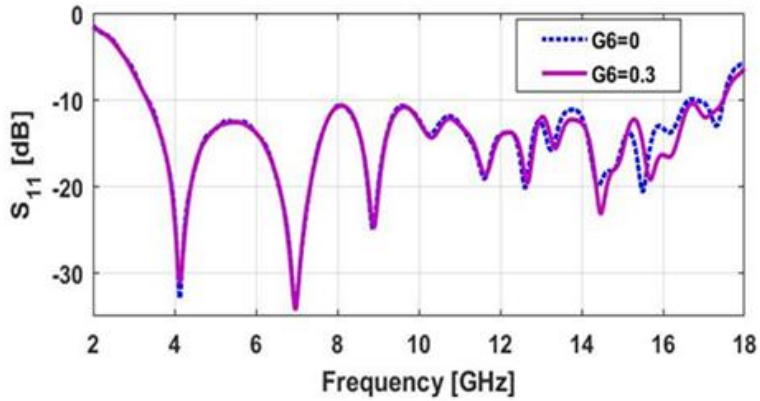

Fig. 7. Parametric study where the value of *G6* was varied.

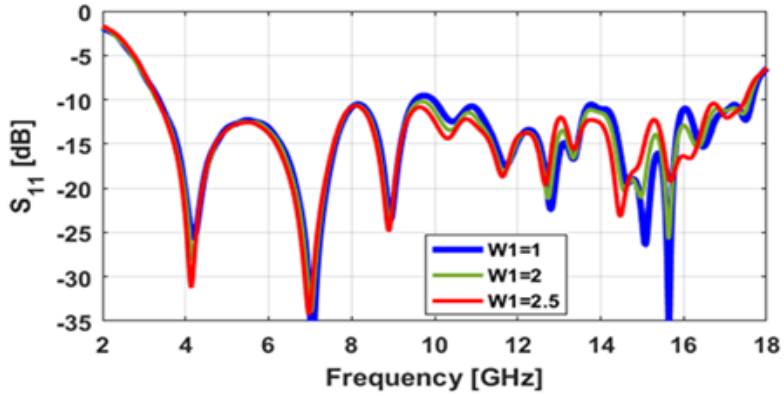

Fig. 8. Parametric study where the value of W_1 was varied.

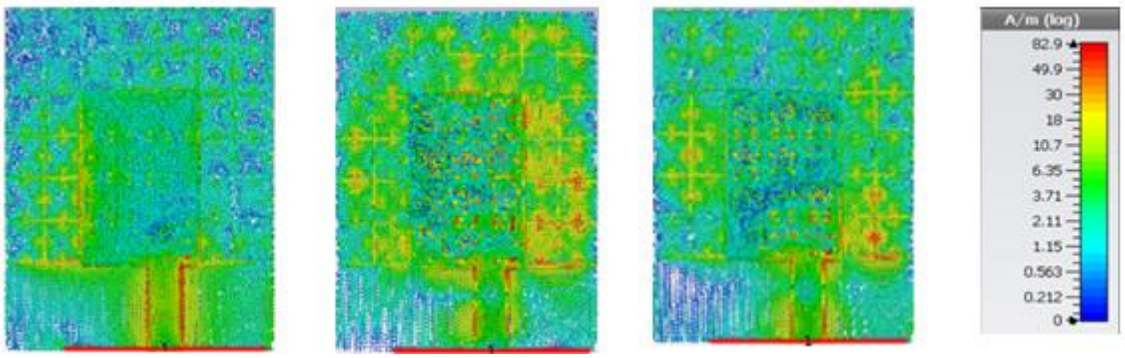

5 GHz 11 GHz 16 GHz

Fig. 9. Surface current distribution of the proposed antenna

To better understand the antenna behavior, the surface current distribution at 5 GHz, 11 GHz, and 16 GHz are illustrated in Fig. 9. It was observed that the current was concentrated on the two edges of the feed line and the bottom section of the radiating structure at low frequency. However, when the frequency was increased, the current distribution began to flow towards the top section of the structure.

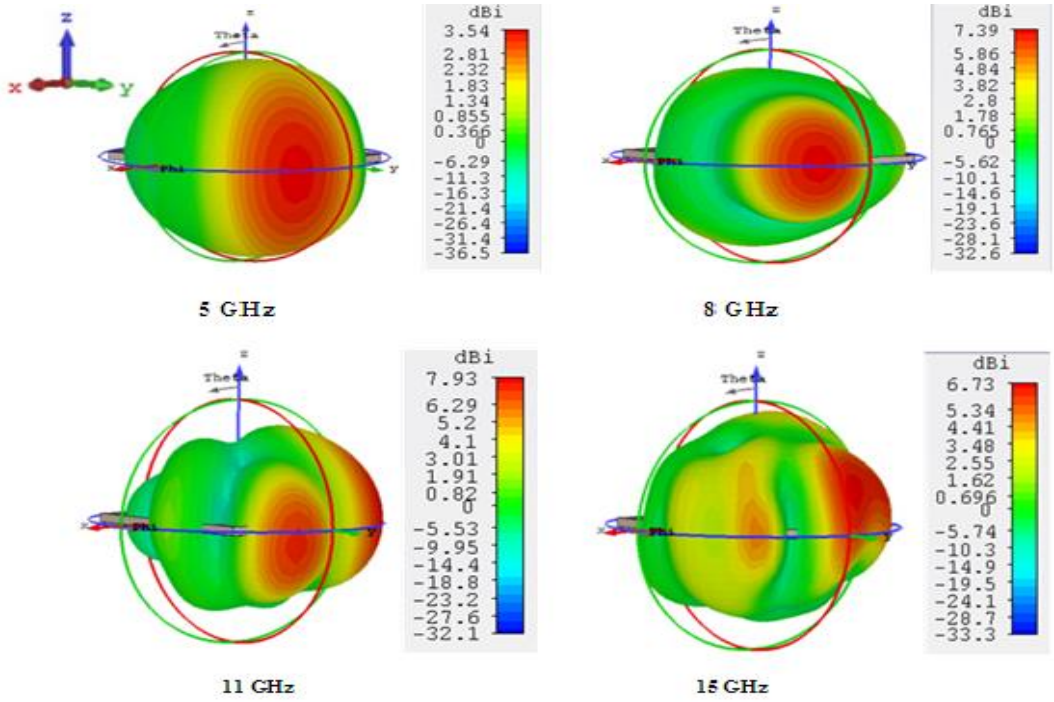

Fig. 10. 3D radiation pattern at different frequencies within the band

The 3-D radiation patterns of the proposed antenna at four different frequencies within the band such as 5 GHz, 8 GHz, 11 GHz, and 15 GHz are shown in Fig. 10. Because of the left-handed transmission properties, the greatest radiation occurred along the horizontal direction rather than vertical direction as in the status of a simple patch antenna. At a lower frequency such as at 5 GHz, the maximum radiation occurred along the vertical direction, with some tilt towards the XY-plane. At a higher frequency (8 GHz, 11 GHz, and 15 GHz) on the other hand, the highest intensity of radiation was along the x-direction because the higher order modes were responsible for the splitting of radiation lobe. In this way, at 11 GHz and 15 GHz, the main beam splitting had its direction of radiation intensity along the x-direction.

V. Measurements and Discussion

The antenna presented was optimized and manufactured using CNC machine, as shown in Fig. 11. The S-parameters were measured using the Agilent Technologies Microwave Analyzer and demonstrated in Fig. 12. The antenna designed was found to have good impedance bandwidth of 136 %, which covered the 3.3 - 17.4 GHz frequency range. Fig. 12 compares the conventional antenna simulation results to the metamaterial-based-UWB antenna simulated and measured results.

Fig. 11. The fabricated antenna and measurement setup

We observed that the antenna without MTM unit cells did not cover the ultra-wideband rang approved by the FCC. The proposed antenna with double layer 2-D periodic pattern on the patch and on the ground attained a

broader bandwidth of about 14.1 GHz when compared with the original antenna.

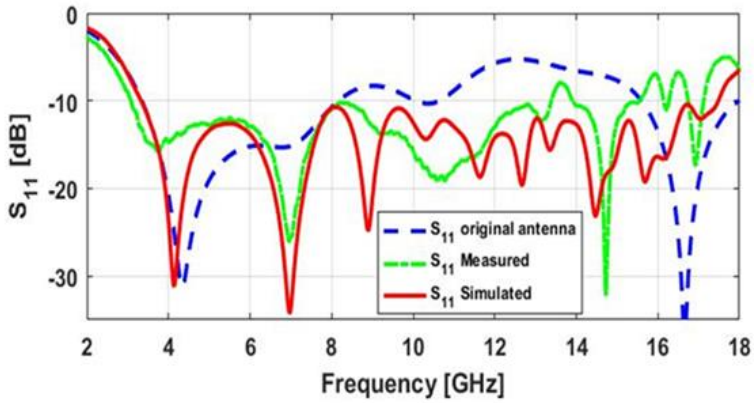

Fig. 12. S-parameters of the conventional antenna and the simulated and measured results of the proposed UWB antenna

The calculated realized gain is plotted in Fig. 13 for the antenna proposed for the frequency range of 3 to18 GHz with an average value of 5.8 dB from 3.3 GHz to 17.4 GHz. The antenna gain reached its maximum level of 6.9 dB at 12.2 GHz and a minimum level of 0.89 dB at 15.3 GHz.

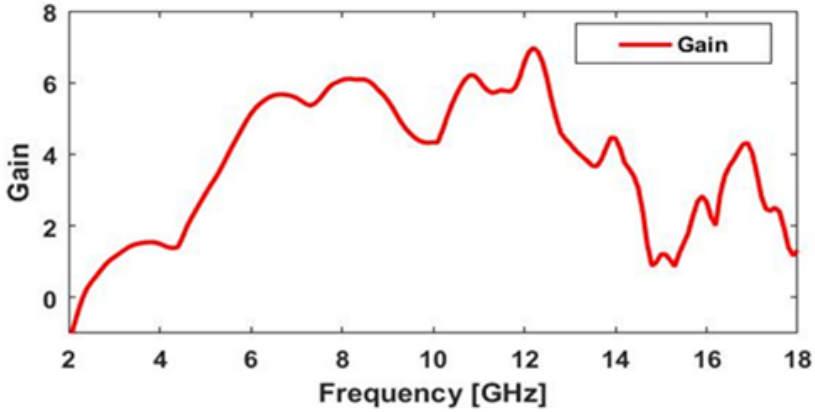

Fig. 13. Simulated gain of the proposed UWB antenna

The simulated radiation patterns in the xy, yz, and xz-planes at three different frequencies within the band, viz. 4.7, 13, 17.3 GHz, are shown in Fig. 14. In view of the left-handed transmission characteristics, strong radiation in the horizontal direction instead of vertical direction was observed, as in the patch antenna. The proposed antenna had a stable radiation pattern almost Omni-directional over the whole band.

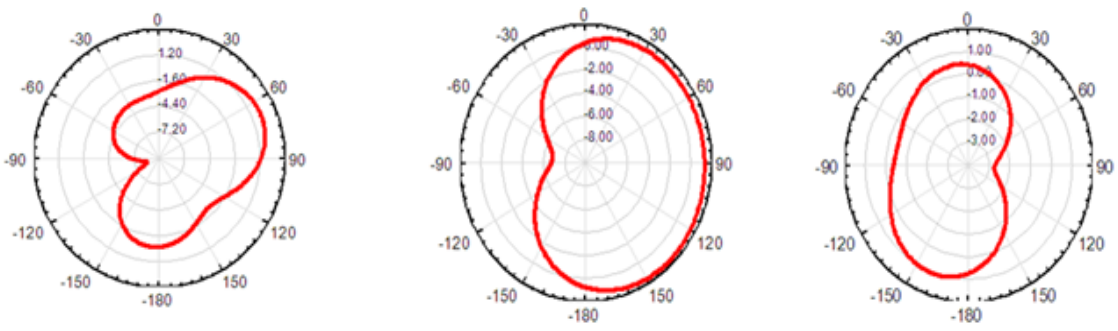

@ 4.7 GHz

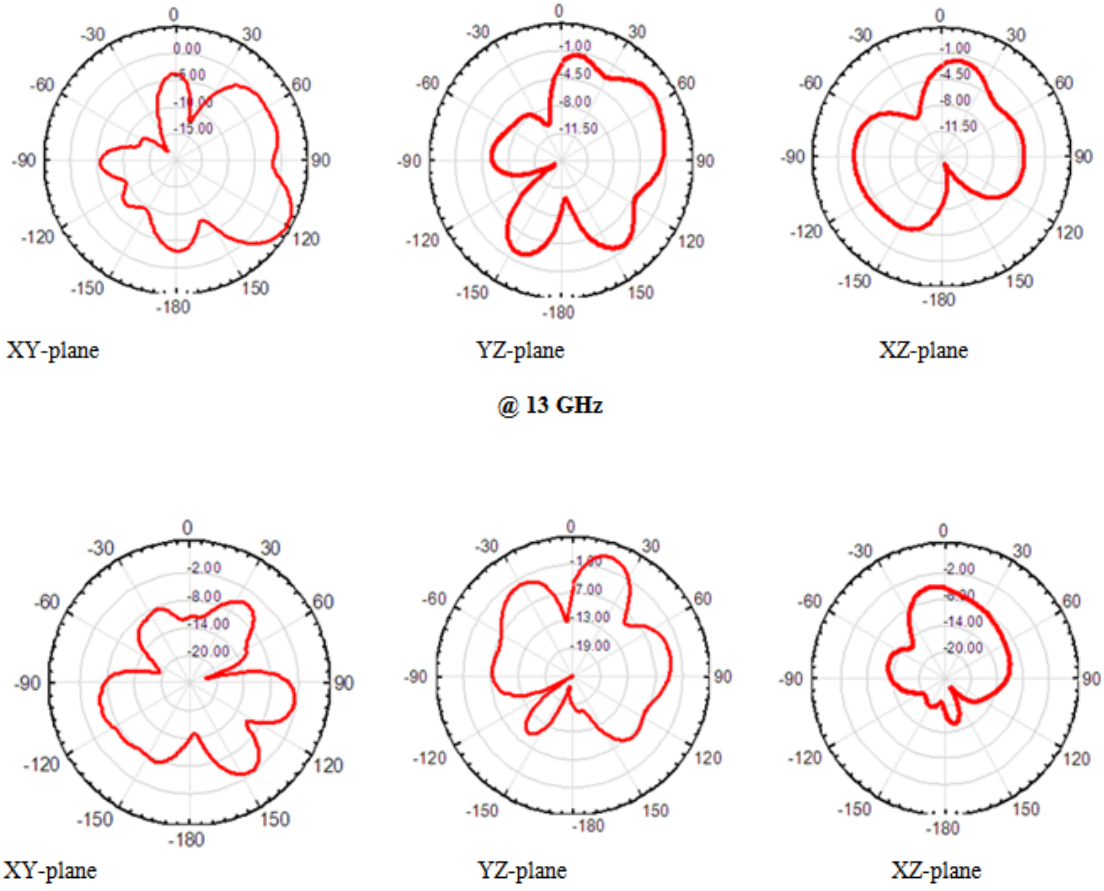

Fig. 14. Simulated radiation pattern for the proposed antenna

VI. Conclusion

A compact UWB antenna using double layer 2D periodic MTM structure is presented. The antenna is designed using the metamaterial concept to enhance the antenna gain and bandwidth by etching a metamaterial unit cell arranged in a 2D pattern on the radiating element and on the bottom ground plane. The antenna has isolated W-shaped slots etched on the ground plane and T-shaped slots etched on the patch. The dimensions of this antenna are 27.6 ×31.8 mm^2 built on 1.6 mm thicknesses FR4 substrate of 4.5 relative permittivity and 0.02 loss tangent. A broad-bandwidth from 3.3 GHz to more than 17 GHz (> 136 %) with an average gain of 5.8 dB over the whole range was achieved. The widening of the bandwidth was based on the concept of radiation of the LHM in a 2D pattern configuration. The radiation attributes of the antenna indicated that most extreme radiation occurred in the horizontal plane and tended towards directional radiation as the frequency increased. This produced a high-gain antenna at higher-frequencies. Because of these good radiation characteristics, the proposed antenna is a good candidate for UWB applications.

References

[1]. Federal Communication Commission. First order and report: revision of part 15 of the commission's rules regarding UWB transmission systems. April 2002.
[2]. Sourabh B., Shweta S., Ved P., Bhaskar N. Study the various feeding techniques of microstrip antenna using design and simulation using CST microwave studio. IJETAE 2014; 4 (9): 318-319.
[3]. Mohamed A. B., Ehab K. I. H., Wael A. A., and Mohamed Z. M. H. Dual-band microstrip antenna for WiMAX applications using complementary split ring resonators. In: 33rd National radio science conference; 22-25 Feb. 2016; Aswan, Egypt. pp. 57-63.
[4]. Ehab K. I. H., Nirmen M. Compact tri-band notched characteristics UWB antenna for WiMax, WLAN, and X-band applications. AEM 2017; 6(2): 54-57.

[5]. M.E.Sundaravel, Vallikannu AL, HimanshuSheker, "Compact Printed Slot UWB Monopole Antenna with Ground Plane Slit," IOSR Journal of Electronics and Communication Engineering (IOSR-JECE).Volume 8, Issue 3, Nov. - Dec. 2013, PP 25-30.
[6]. M. Al-Husseini, A. Ramadan, Y. Tawk, A. El-Hajj, K.Y. Kabalan. Design and ground plane optimization of a CPW-fed ultra-wideband antenna. Turk J ElecEng& Comp Sci 2011; 19: 243-250.
[7]. Leila Y., Baharak M.-I., and Omar M. R.. Enhanced bandwidth artificial magnetic ground plane for low-profile antennas. IEEE Antennas Wireless Propag. Lett. 2007; 6 (10): 289–292.
[8]. Pues, H. F., and A. Van de Capelle. An ımpedance-matching technique for ıncreasing the bandwidth of microstrip antennas. IEEE Trans. Antennas Propag. 1989; 37 (11): 1345 - 1354.
[9]. Gaurav K.P., Hari S.S., Pradutt K.B., and Manoj K.M. Metamaterial based compact antenna design for UWB applications. In: IEEE Region 10 Symposium; 2014; pp.15-17.
[10]. Neelam S., Rekha C. A review paper on techniques and design for metamaterial absorber. IJSER 2015; 6 (10): 60-64.
[11]. Y. Hao and R. Mittra. FDTD of metamaterial: Theory and Application. 1st edArtech House Publishers, 2008.
[12]. F. Capolino. Theory and phenomena of metamaterial. 1st ed. Taylor & Francis, 2009.
[13]. Simovski, R., P. A. Belov, and H. Sailing. Backward wave region and negative material parameters of structure formed by lattices of wires and split-ring resonators. IEEE Trans. Antennas Propag. 2003; 51 (10): 2582-2591.
[14]. Salim L., Roman K., and Miroslaw C. Bandwidth enhancement of a microstrip patch antenna using the metamaterial planar periodic structure. In: PIERS Proceedings, July 2015.
[15]. L. W. Li, Y. N. Li, T. S. Yeo, J. R. Mosig, and O. J. F. Martin. A Broadband and high-gain metamaterial microstrip antenna. ApplPhysLett 2010; 96: 164101.
[16]. X. Han, H. J. Song, Z. Q. Yi, J. D. Lin. Compact ultra-wideband microstrip antenna with metamaterials. Chin. Phys. Lett. 2012; 29 (11).
[17]. D. Sievenpiper, L. Zhang, R.F. Jimenez Broas, N.G. Alexopoulos, and E. Yablonovitch. High-ımpedance electromagnetic surfaces with a forbidden frequency band. IEEE Trans. Microw. Theory Techn. 1999; 47 (11): 2059-2074.
[18]. Li Y., Mingyan F., Fanglu Ch., Jingzhao S., Zhenghe F. A novel compact electromagnetic-bandgap (EBG) structure and ıts applications for microwave circuits. IEEE Trans. Microw. Theory Techn. 2005; 53 (1): 183-190.

IOSR Journal of Electronics and Communication Engineering (IOSR-JECE) is UGC approved Journal with Sl. No. 5016, Journal no. 49082.

Gehad Nady, Ehab K. I. Hamad, "Design of Compact UWB Microstrip Antenna Using Double-Layer 2D Periodic Structure," *IOSR Journal of Electronics and Communication Engineering* (IOSR-JECE) 13.4 (2018): 76-84.